Towards trapping of molecular ions in a linear Paul Trap

Emil Lenler-Eriksen

PhD Progress Report

Department of Physics and Astronomy
Aarhus University

May 2024

Abstract

An abstract...

Colophon

Towards trapping of molecular ions in a linear Paul Trap

PhD progress report by Emil Lenler-Eriksen.

The PhD project is supervised by Michael Drewsen

Typeset by the author using LaTeX and the memoir document class, using Linux Libertine and Linux Biolinum 11.0/13.6pt.

Contents

Chapter 1

Introduction

In the 1950's Wolfgang Paul invented the so-called Paul trap, for trapping charged particles within a quadrupolar electromagnetic field.CITE. In 1989 he would go on to recieve the Nobel Prize in physics, alongside Hans Dehmelt, "for the development of the ion trap technique" CITE. With the many technological and scientific advancements since the Paul trap's inception, among which the laser is an especially important one, it is now possible to trap, and cool single ions to temperatures below 1mK CITE Wineland. Such cold ions pose many interesting possibilities for science, as they can make good candidates for atomic clocks CLOCK, or the basis for quantum computers Wineland, Cirac Zoller.

Paul traps are also used for the study of fluorescence of molecules in the gas phase CITE Steen?, where pulsed lasers can be used to excite large clouds of molecular ions, whose fluorescence spectrum may then be recorded and studied. However as most molecules lack the necessary energy level structure for laser cooling, the temperature of these experiments are limited by their cryogenic cooling environment.

The aim of my PhD thesis is to build an experiment where single molecular ions from an electrospray ionization source FENN can be trapped in a linear Paul trap alongside a Ba^+ ion and cooled to their motional ground state. In such a setup we would like to investigate the molecules using a method called photon recoil spectroscopy CITE EMILIE. This method functions by using the momentum kick associated with the molecules absorption of light as a measure of whether absorption has occured, and is explained further in chapter 5. Directly applying this method to two-ion systems with large mismatches in mass and charge is challenging, since the motions of the ions are only very weakly coupled, and thus the absorption kick will predominantly excite the motion of the molecule, which is not sensitive to the readout performed by a laser on the Ba^+ ion. Due to this issue I have been looking at CITE, and developing theory for how to transfer energy from one motional mode to another, to allow for efficient readout of the absorption kick.

Outline of the report

The report is divided into 6 different chapters. Chapter 1 is a brief introduction to the field, some of the challenges I face, and what I hope to accomplish with my PhD.

Chapter 2 describes the physics of trapping ions in a linear Paul trap and is split into two sections, the first describing the trapping of a single ion, while the latter derives the common motion of two ions in the trap.

Next is chapter 3 which describes the electrospray ionization source, which is the source of molecular ions for the experiment. The first section of this chapter is an overview of the setup and the second contains a characterization of one of the octopoles guides within the setup.

After that I move on to chapter 4 which describes the laser cooling necessary for eventually reaching the motional ground state of a two-ion system. The first section contains the theory for doppler cooling, which allows the ions to reach a temperature of ~1mK. The second section describes sideband cooling, which is necessary to cool the motion of the system to its quantum mechanical ground state. Finally the 3rd section of this chapter talks on how one can couple the motion of the ions by using fx. an external field, in order to improve the cooling of systems where the two ions have large differences in mass and charge.

Finally chapter 6 gives a short plan of the work I plan to do in the latter half of my PhD studies here at Aarhus.

Chapter 2

The Linear Paul Trap

2.1 Single ion in a linear Paul Trap

The linear Paul trap consists of four rods, each of which is split into three electrodes as is seen on fig. 2.1. The coordinate system for the trap is defined such that the z-axis runs down along the centre of the trap, while the x, y-axes go between diagonally opposed rods. Furthermore we define z_0 to be half the length of center electrodes, while we define r_0 as half the distance between diagoanlly opposed electrodes as seen on fig. 2.1. In order to trap an ion along the z-direction a static voltage V_{end} is applied to all of the electrodes on the end of the rods. By applying such a votlage to these endcap electrodes an electrical potential is generated, which in the region around the centre of the trap can be written as

$$\phi_{DC}(z) = \frac{\kappa V_{end}}{z_0^2} z^2, \tag{2.1}$$

where κ is a constant defined by the specific geometry of the trap, and z is the position of the ion along the z axis. Thus an ion of mass m and charge Q finds itself sitting in a harmonic potential

$$V_{DC}(z) = \frac{1}{2} m \omega_z^2 z^2, \quad \omega_z = \sqrt{\frac{2Q\kappa V_{end}}{m z_0^2}}, \tag{2.2}$$

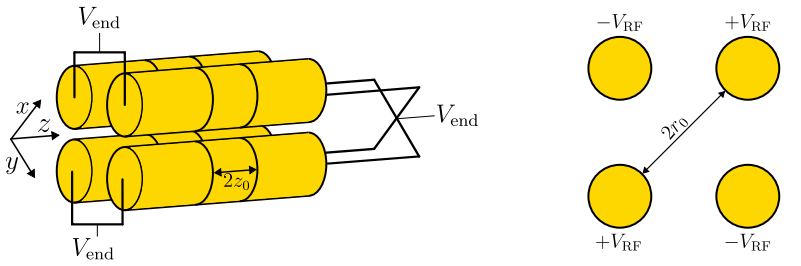

Figure 2.1: Example schematic of a linear paul trap showing: (left) a 3D model of the paul Trap with both the DC endcap voltages applied. (right) an end-view down the Paul trap, showing the phase of the RF voltages applied to the different rods..

where ω_z is the frequency of the ions oscillating motion along the z-axis.

For the radial directions it is necessary to take a slightly different approach, indeed Earnshaw's theorem Earnshaw states that it is impossible to trap a charged particle in all three directions, solely through the use of electrostatic forces. If we look at the electrical potential in the x, y-plane from the DC endcaps we also find

$$\phi_{DC}(x, y) = -\frac{\kappa V_{end}}{2z_0^2}(x^2 + y^2), \tag{2.3}$$

which is clearly repulsing the ion from the center of the trap.

To counteract this repulsive effect, we employ an RF voltage, oscillating at frequency Ω_{RF}, with an amplitude V_{RF} on all four rods. Neighbouring rods have opposites phases while, dioganlly opposing rods share a phase, as seen on fig. 2.1. We can then write the total time dependant electrical potential in the x, y-plane as KARIN

$$\phi(x, y, t) = -\frac{\kappa V_{end}}{2z_0^2}(x^2 + y^2) - \frac{V_{RF}}{2r_0^2}(x^2 - y^2)\cos(\Omega_{RF} t), \tag{2.4}$$

where the first term comes from the repulsing DC potential, and the second term comes from the RF voltages applied to the rods.

The equations of motion in the radial plane can be rewritten on a more compact form by adopting the notation

$$\tau = \frac{\Omega_{RF} t}{2}, \quad a = -\frac{4Q\kappa V_{DC}}{mz_0^2\Omega_{RF}^2}, \quad q_x = -q_y = \frac{2QV_{RF}}{mr_0^2\Omega_{RF}^2}, \tag{2.5}$$

which allows for the equations of motion to be written as

$$\frac{\mathrm{d}^2\gamma}{\mathrm{d}\tau^2} + (a - 2q_\gamma\cos(2\tau))\gamma, \quad \gamma \in \{x, y\}. \tag{2.6}$$

Equation (2.6) is known as the Mathieu equation CITE, the Mathieu equation has bounded solutions for several sets of (a, q_γ) parameters, however, the conditions usually used in experiment state that for a given value of q_γ, a must be found between the two curves approximated by CITE

$$a_0(q_\gamma) \approx -\frac{1}{2}q_\gamma^2 + \frac{7}{128}q_\gamma^4 - \frac{29}{2304}q_\gamma^6 + \frac{68687}{18874368}q_\gamma^8, \tag{2.7}$$

$$b_1(q_\gamma) \approx 1 - q_\gamma - \frac{1}{8}q_\gamma^2 + \frac{1}{64}q_\gamma^3 - \frac{1}{1536}q_\gamma^4 - \frac{11}{36864}q_\gamma^5. \tag{2.8}$$

Together these two lines form what is known as a stability diagram. Since a positive DC voltage is needed for the confinement in the axial direction, we usually confine ourselves to considering stability in the $a < 0$ region. A plot of the stable region for the linear Paul trap can be see on fig. 2.2

In the case where $|a|, |q_\gamma| \ll 1$ the solution to eq. (2.6) can be approximated to

$$\gamma(t) = \gamma_0\left(1 - \frac{q_\gamma}{2}\cos(\Omega_{RF} t)\right)\cos(\omega_r t), \quad \omega_r = \frac{\Omega_{RF}}{2}\sqrt{\frac{q_\gamma^2}{2} + a}. \tag{2.9}$$

Since $|q_\gamma| \ll 1$ we see that there is a large-amplitude motion of the ion at frequency ω_r. This motion is typically referred to as secular motion in the litterature. The

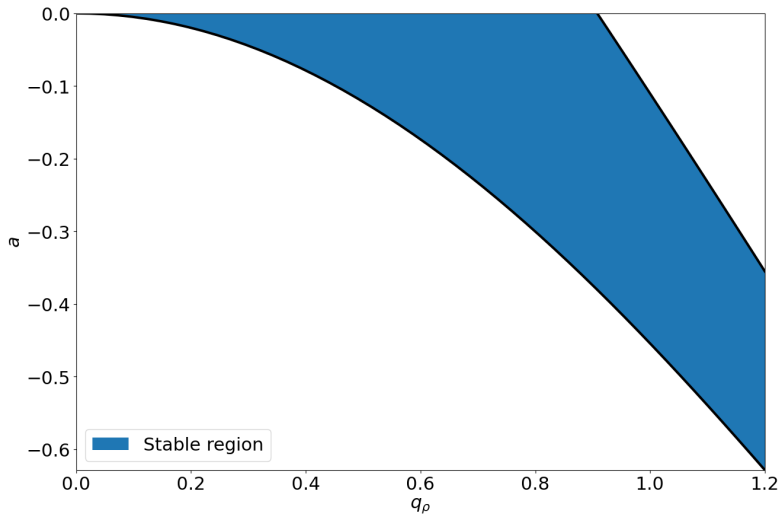

FIGURE 2.2: Plot of the Mathieu stability diagram for negative values of a. The blue colored area contains the set of bounded, and thus stable solution to the Mathieu equation of eq. (2.6).

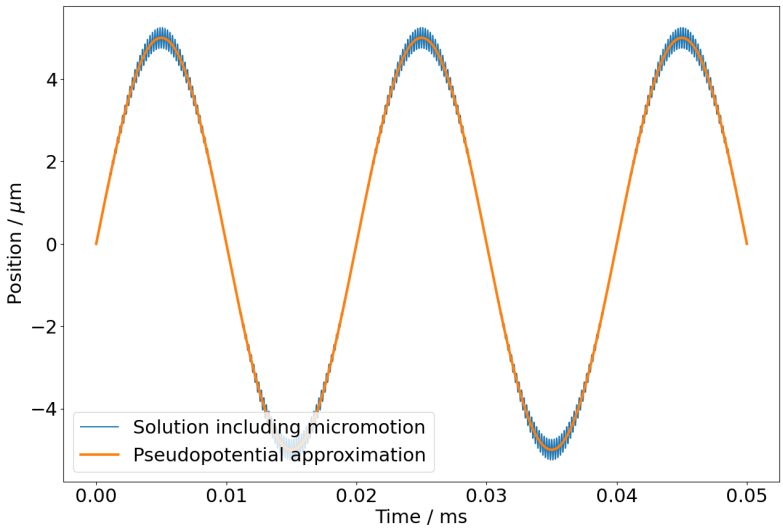

FIGURE 2.3: Trajectories including (blue) micromotion or calculated through the pseudopotential approximation (orange), for $\gamma_0 = 5\mu$m, $\omega_r = 2\pi \times 50$kHz, $\Omega_{RF} = 2\pi \times 5.2$MHz..

frequency ω_r is much slower than the RF frequency of the trap (typically 10's-100's of kHz vs. 5MHz in the case of our trap).

In addition there is a small-amplitude motion superimposed on top, oscillating at the RF frequency. This motion is typically referred to as micromotion. Thus the full picture we now get, is one of the ion performing slow, but large oscillations in the radial plane, with an additional micromotion on top. An example trajectory can be seen on fig. 2.3, where the micromotion is clearly visible.

It is common to average over the micromotion of the ion, keeping only the term oscillating at ω_r. If this is done, it is clear that the ion then moves as if in an effective

potential (often referred to as pseudopotential in the litterature) given by

$$V_{Pseudo}(\gamma) = \frac{1}{2} m \omega_r^2 \gamma^2, \quad \gamma \in \{x, y\}. \tag{2.10}$$

The pseudopotential approximation is especially useful when working with trapped ions in a quantum mechanical regime, since their Hamiltonian is then simply that of a harmonic oscillator, which is one of the most well-studied examples in all of quantum mechanics.

2.2 Two ions in a linear Paul trap

We now move on to the topic of two co-trapped ions in a Paul trap. We shall denote the ions 1 and 2 respectively, with masses m_1, m_2, and charges Q_1, Q_2. Remembering to include the Coulomb interaction between the two ions, the potential energy of the system, in the pseudopotential approximation, can then be written as

$$\begin{aligned} V(\boldsymbol{r_1}, \boldsymbol{r_2}) =& \frac{1}{2} m_1 \left(\omega_{1,z}^2 z_1^2 + \omega_{1,r}^2 (x_1^2 + y_1^2) \right) + \frac{1}{2} m_2 \left(\omega_{2,z}^2 + \omega_{2,r}^2 (x_2^2 + y_2^2) \right) \\ &+ \frac{Q_2 Q_2}{4\pi\epsilon_0} \frac{1}{|r_1 - r_2|}, \end{aligned} \tag{2.11}$$

where $\omega_{j,(r/z)}$ is calculated as in eqs. (2.2) and (2.9), using the mass and charge of ion j. For the rest of the derivations in this report we are, unless otherwise noted, going to ignore the y part of motion of the ions since our system exhibits a radial symmetry, and thus any equations that hold for x will hold for y as well.

We shall first derive the equilibrium positions for the two ions. Assuming the radial trapping is stronger than the axial trapping we know that the ions will along themselves along the z-axis, and thus we slightly simplify the potential to be minimized

$$V(z_1, z_2) = \frac{1}{2} m_1 \omega_{1,z}^2 z_1^2 + \frac{1}{2} m_2 \omega_{2,z}^2 z_2^2 + \frac{Q_1 Q_2}{4\pi\epsilon_0} \frac{1}{z_1 - z_2}, \tag{2.12}$$

where we assume without loss of generality that $z_1 > z_2$. Taking the derivatives with respect to the ion coordinates to be zero we find

$$\frac{\partial V}{\partial z_1} = m_1 \omega_{1,z}^2 z_{1,eq} - \frac{Q_1 Q_2}{4\pi\epsilon_0} \frac{1}{(z_{1,eq} - z_{2,eq})^2} = 0, \tag{2.13}$$

$$\frac{\partial V}{\partial z_2} = m_2 \omega_{2,z}^2 z_{2,eq} + \frac{Q_1 Q_2}{4\pi\epsilon_0} \frac{1}{(z_{1,eq} - z_{2,eq})^2} = 0, \tag{2.14}$$

where the (eq) subscript denotes the value is taken at the equilibrium position. Adding the two together we find

$$z_{1,eq} = -\rho z_{2,eq}, \tag{2.15}$$

where $\rho = \frac{Q_2}{Q_1}$ is the charge ratio between the two ions. It is interesting to note that the equilibrium positions are entirely independent on the masses of the ions. We can now plug this relationship back into eq. (2.13) to find an expression for $z_{1,eq}$

$$z_{1,eq} = \left(\frac{Q_1 Q_2}{4\pi\epsilon_0 m_1 \omega_{1,z}^2} \frac{1}{(1 + \frac{1}{\rho})^2} \right)^{1/3}, \tag{2.16}$$

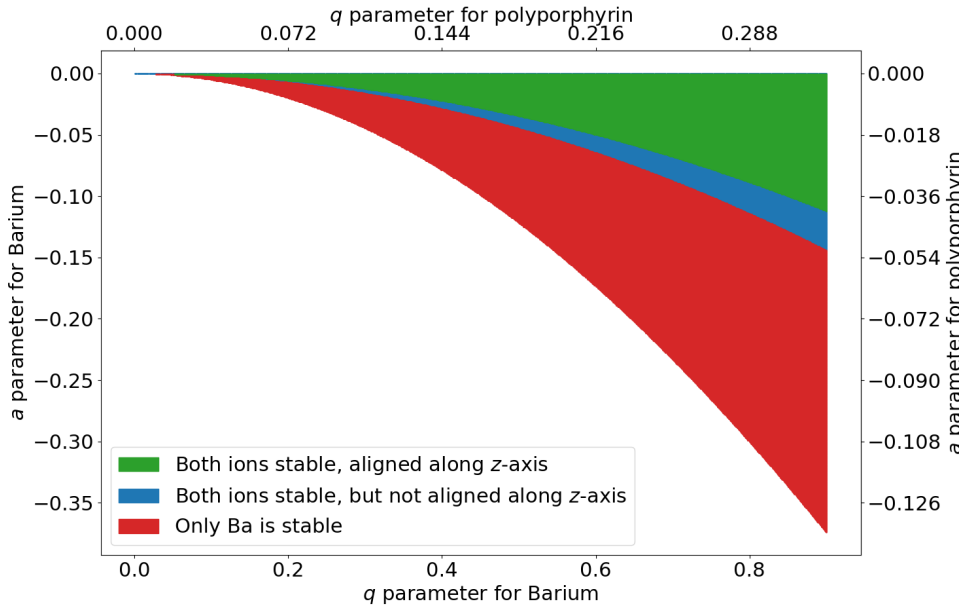

FIGURE 2.4: Stability diagram for Ba^+ cotrapped alongside a polyporphyrin system, holding 12 porphyrin rings with 2 charges each for a total of $m_2 = 9000$amu, $Q_2 = 24$e. The green area represents the a and q parameters ideal for experiments as both ions have stable trajectories, while they also align along the z-axis. for trapping parameters that fall within the blue area the ions have stable trajectories, but will aliugn along the radial axes. Finally the red shaded area describes the parameters for which only the Ba^+ ion has stable trajectories. It is thus clear that trapping two ions with very different mass-to-charge ratios puts considerable additional bounds on the stability of the system..

it has to be noted that if one expands the $\omega_{1,z}$ factor in the denominator one finds that the equilibrium position is mass independent. This has not been done here, as it lengthens the expression considerably.

In this derivation we assumed that the ions aligned themselves along the z-axis, which is also the desired case. However one of course has to design any experiment such that the voltages applied result in such an orientation. This leads to further "stability" requirements for the two-ion system. Following the derivation above one can similarly find expressions for equilibrium positions along the x-axis. The ions will naturally align themselves along the axis which has the lowest energy at equilibrium. Through much massaging, one finds, that if the ions are to align along z, the follow inequality must hold:

$$\frac{m_1 m_2 \omega_{1,z}^2 \omega_{2,z}^2}{m_1 \omega_{1,z}^2 + m_2 \omega_{2,z}^2} < \frac{m_1 m_2 \omega_{1,r}^2 \omega_{2,r}^2}{m_1 \omega_{1,r}^2 + m_2 \omega_{2,r}^2}. \tag{2.17}$$

In addition to this, the ions must also uphold the stability criterium outlined in section 2.1. Given that both ions need to be stable *and* trapped along the z-axis the new stability diagram can look considerably different. An example for a polyporphyrin of mass 9000amu and charge 24e trapped alongside Ba^+ is seen on fig. 2.4.

With the equilibrium positions of the ions, and the criteria for them to be stably trapped determined. One can now determine the new oscillation frequencies of the ions. To do this we reintroduce the full potential of eq. (2.11) and perform a Taylor expansion to 2nd order around the equilibrium position of the system. When performing calculations of vibrational modes for coupled oscillators it is common to introduce mass-weighted displacement coordinates defined as

$$\xi_1 = \sqrt{m_1}(z_{eq,1} - z_1), \quad \xi_2 = \sqrt{m_2}(z_{2,eq} - z_2), \quad \xi_3 = \sqrt{m_1}x_1, \quad \xi_4 = \sqrt{m_2}x_2. \tag{2.18}$$

If we write up the Lagrangian for the system in this coordinate system we find

$$\mathcal{L} = \sum_{i=1}^{4} \dot{\xi}_i^2 - \frac{1}{2}\sum_{i=1}^{4} K_{ij}\xi_i\xi_j, \tag{2.19}$$

where $K_{ij} = \left(\frac{\partial^2 V}{\partial r_i \partial r_j}\bigg|_{eq} / \sqrt{m_i m_j} \right)$ and $\{r_1, r_2, r_3, r_4\} = \{z_1, z_2, x_1, x_2\}$. It should be noted that the Taylor expansion in principle also adds an energy offset corresponding to the potential energy when the system is in equilibrium. We ignore this offset as it introduces no dynamics.

Explicit calculation of the K_{ij} terms grants several zero's. The non-zero K_{ij}'s evaluate to

$$K_{11} = \omega_{1,z}^2\left(1 + \frac{2}{1+1/\rho}\right), \tag{2.20}$$

$$K_{12} = K_{21} = -\frac{2\omega_{1,z}^2}{\sqrt{\mu}(1+1/\rho)}, \tag{2.21}$$

$$K_{22} = \omega_{1,z}^2\frac{\rho}{\mu}\left(1 + \frac{2}{1+\rho}\right), \tag{2.22}$$

$$K_{33} = \omega_{1,r}^2 - \frac{\omega_{1,z}^2}{1+1/\rho}, \tag{2.23}$$

$$K_{34} = K_{43} = -\frac{1}{2}K_{12}, \tag{2.24}$$

$$K_{44} = \omega_{2,r}^2 - \frac{\omega_{1,z}^2}{\mu(1+1/\rho)}. \tag{2.25}$$

The coupled motional modes as well as their oscillation frequencies can now be found by diagonalizing the matrix TAYLOR

$$K = \begin{bmatrix} K_{11} & K_{12} & 0 & 0 \\ K_{21} & K_{22} & 0 & 0 \\ 0 & 0 & K_{33} & K_{34} \\ 0 & 0 & K_{43} & K_{44} \end{bmatrix}, \tag{2.26}$$

which is block diagonal. This simplifies the problem significantly, as it suffices to solve the eigenproblem for the two 2x2 matrices on the diagonal

$$K_z = \begin{bmatrix} K_{11} & K_{12} \\ K_{21} & K_{22} \end{bmatrix}, \quad K_r \begin{bmatrix} K_{33} & K_{34} \\ K_{43} & K_{44} \\ , & \end{bmatrix} \tag{2.27}$$

which will give the solutions for the axial and radial motion respectively. Solving the probem yields two modes for each direction, one where the ions move together in-phase with one another (sometimes referred to as the center-of-mass mode), and one where they move out of phase (sometimes referred to as the breathing mode). For the frequencies one finds

$$\left(\omega_z^{i/o}\right)^2 = \frac{K_{11} + K_{22} \mp \sqrt{(K_{11} - K_{22})^2 + 4K_{12}^2}}{2}, \tag{2.28}$$

$$\left(\omega_r^{i/o}\right)^2 = \frac{K_{33} + K_{44} \pm \sqrt{(K_{33} - K_{44})^2 + 4K_{34}^2}}{2}. \tag{2.29}$$

Expanding the K_{ij}'s above would make the equations considerably harder to read, and as such is not done here. Denoting the normalized eigenmodes for the axial motion as $\boldsymbol{\alpha_{i/o}}$, and the ones for radial motion $\boldsymbol{\beta_{i/o}}$ one finds

$$\boldsymbol{\alpha_{i/o}} = \frac{1}{\sqrt{1 + \tilde{\alpha}_{i/o}^2}} \begin{pmatrix} \tilde{\alpha}_{i/o} \\ 1 \end{pmatrix}, \quad \tilde{\alpha}_{i/o} = \frac{\left(\omega_z^{i/o}\right)^2 - K_{22}}{K_{12}}, \tag{2.30}$$

$$\boldsymbol{\beta_{i/o}} = \frac{1}{\sqrt{1 + \tilde{\beta}_{i/o}^2}} \begin{pmatrix} \tilde{\beta}_{i/o} \\ 1 \end{pmatrix}, \quad \tilde{\beta}_{i/o} = \frac{\left(\omega_r^{i/o}\right)^2 - K_{44}}{K_{34}}. \tag{2.31}$$

Here the first component of the vector describes the amplitude, often referred to as the contribution or participation, of ion 1 in the motional mode, while the 2nd component of the vector describes the participation of ion 2.

For ions with very different charge-to-mass ratios one finds that the motion of the ions becomes essentially uncoupled. As an example we consider once again a Ba^+ ion trapped alongside a polyporphyrin ($m_2 = 9000$amu, $Q_2 = 24$e), here the axial eigenvector for the in-phase motion is $\boldsymbol{\alpha_i} = (0.092, 0.99)$. Thus the in-phase motion of this system consists of almost exclusively motion of the heavy polyporphyrin. This decoupling of motion has significant consequences for cooling, as will be seen in chapter 4.

Further expansion of the equations above makes them considerably harder to read, and thus is not done here. However, it is good to note that, roughly, one finds that $\tilde{\alpha}_{i/o} \propto \rho/\mu$, while $\tilde{\beta}_{i/o} \propto (\rho/\mu)^2$. This means the decoupling of the ion motion tends to be larger along the radial direction as the charge and mass ratios of the two ions become more skewed.

Chapter 3

Electrospray ionization source

3.1 Overview of the electrospray and its components

3.2 Experiments on the first octopole

Chapter 4

Cooling

4.1 Doppler cooling

4.2 Sideband Cooling

4.3 Coupling of motional modes to enhance cooling

Chapter 5

Photon Recoil Spectroscopy (WHERE SHOULD THIS GO?)

Chapter 6

Future Work

In the following, I will outline the topics I will work on in the final part of my PhD …